Chapter 1

Introduction

Understanding the physical processes which shaped our Universe is the fundamental goal of all fields in Astrophysics. A successful theory of the Universe must describe how it evolved from the primordial soup of matter present just after the Big Bang to the multitude of galaxy properties we see today.

The most widely accepted cosmological model is the Λ-CDM (Λ- cold dark matter) model which describes a flat Universe made of only $\sim 5\%$ baryonic ("normal") matter, $\sim 26\%$ cold dark matter and $\sim 69\%$ dark energy (Planck Collaboration, 2016). In such a Universe, tiny quantum fluctuations in the early Universe grow with time, becoming overdense and laying the foundations for galaxy formation (Guth & Pi, 1982; Hawking, 1982; Linde, 1982; Starobinsky, 1982). Given the relatively small fraction of baryonic matter in the Universe, its gravitational contribution to this process is often neglected, greatly simplifying the problem. Structure in simulations is then observed to form hierarchically (Press & Schechter, 1974; Gott & Rees, 1975; White & Rees, 1978; Aarseth et al., 1979; Gott et al., 1979; Turner et al., 1979; Efstathiou & Eastwood, 1981; Davis et al., 1985). At the overdense regions in the early Universe, matter collapses dissipationally under its own gravity forming a dark matter 'halo', which then grows through smooth accretion and mergers of other halos to produce the large scale structure of galaxy filaments, clusters and voids we observe today (see comprehensive review by Frenk & White, 2012).

Adding in localised baryonic physics into this picture however, complicates matters. Galaxies are, unfortunately, not just simple smooth dark matter halos; they are

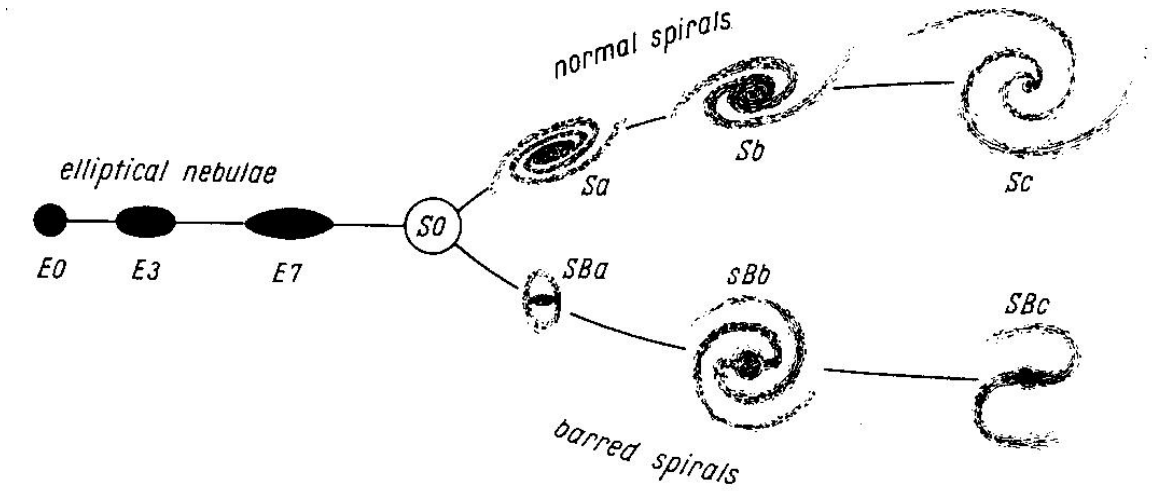

Figure 1.1: The Hubble sequence of galaxy morphology shown on his famous 'tuning fork diagram' as published in Hubble (1936).

thought to start life when baryons cool and condense at the centre of a dark matter halo. Further accretion of matter will cause a gravitational collapse (if angular momentum is present as a result of tidal torques then a rotating gas disc will form Fall & Efstathiou, 1980; Barnes & Efstathiou, 1987), and stars will form as hydrogen gas cools and coalesces. From this moment a galaxy will evolve, its shape changing depending on its encounters (or lack thereof) with other galaxies.

Today we observe galaxies of a multitude of shapes, or morphologies, across all redshift ranges. Hubble (1936) classified galaxies based on their shape, producing the widely adopted 'tuning fork diagram', now known as the Hubble sequence and shown in Figure 1.1. Hubble noticed that galaxies could by broadly categorised as either elliptical in shape or as a disc with spiral arms and/or barred structures. He referred to these categories as early-types (placed to the left of his diagram, in keeping with time axis conventions) and late types respectively, as he thought that as galaxies evolved they developed spiral structure. However, as discussed above, cosmological studies have concluded that galaxies start life as a rotating gas disc and so instead, Hubble's diagram is often read from right to left (with some debate over the placement of the S0 galaxies in this picture; Kormendy & Bender, 1996). Connecting this picture of pure gas disc galaxies in their infancy with the plethora of galaxy structures we see today, is the focus of this thesis.

However, the structure alone is not enough to describe a galaxy's evolution. The magnitude (used as a proxy for stellar mass), star formation rate (SFR), metallicity

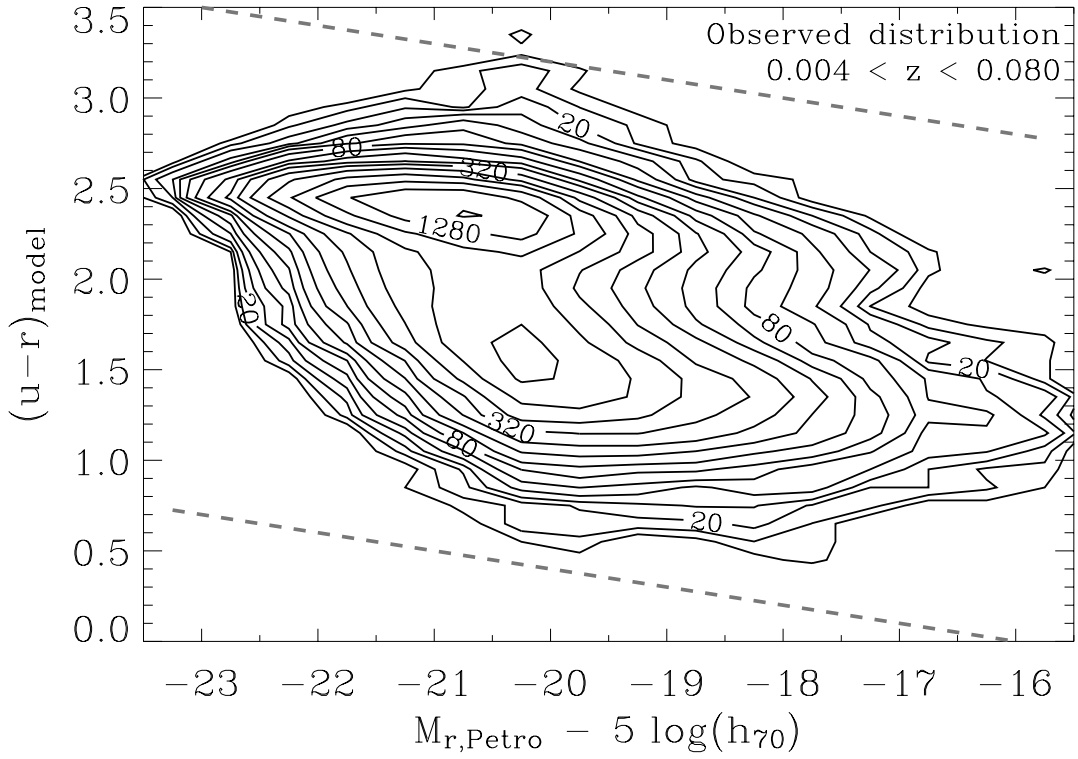

Figure 1.2: The galaxy colour magnitude diagram as observed by Baldry et al. (2004). The figure has been adapted from Figure 1 in Baldry et al. and annotated to show the locations of the red sequence and blue cloud. A lower magnitude corresponds to a higher mass and a large $u - r$ value corresponds to a redder colour.

(Z) and environment are all crucial to describing a galaxy's current state. By studying these galaxy properties, insight into the processes which govern galaxy evolution can be gained.

Large scale surveys of galaxies have first revealed a bimodality in the optical colour-magnitude diagram (CMD) of galaxies finding two distinct populations (see Figure 1.2); one at relatively low mass, with blue optical colours and another at relatively high mass, with red optical colours (Baldry et al., 2004, 2006; Willmer et al., 2006; Ball et al., 2008; Brammer et al., 2009). These populations were dubbed the 'blue cloud' and 'red sequence' respectively (Chester & Roberts, 1964; Bower et al., 1992; Bell et al., 2004; Driver et al., 2006; Faber et al., 2007). The sparsely populated colour space between these two populations was dubbed the 'green valley'.

The majority of disc galaxies were found in the blue cloud and the majority of ellipticals on the red sequence, with colour often used as a proxy for morphology. The Galaxy Zoo project (Lintott et al., 2008, 2011), which produced morphological classifications for a million galaxies, helped to confirm that this colour bimodality is not entirely morphology driven (Strateva et al., 2001; Salim et al., 2007; Schawinski et al., 2007a; Constantin et al., 2008; Bamford et al., 2009; Skibba et al., 2009), detecting larger numbers of spiral galaxies in the red sequence (Masters et al., 2010a) and elliptical galaxies in the blue cloud (Schawinski et al., 2009) than had previously been observed.

Second, large galaxy surveys revealed that star forming galaxies are also observed to lie on a well defined 'star forming sequence' (SFS) in the stellar mass vs. star formation rate (SFR) plane (Brinchmann et al., 2004; Salim et al., 2007; Daddi et al., 2007). The majority of blue cloud galaxies are found to lie on this SFS with the majority of the red sequence lying well below it with very low SFRs. The intermediate colours of the green valley have therefore been interpreted as evidence of recent suppression of star formation (SF; Salim et al., 2007). This suppression of SF and subsequent transition of a galaxy from blue cloud to red sequence must therefore also be intrinsically tied with a possible change in morphology from a disc galaxy to an elliptical galaxy.

The discovery of the fundamental plane (Dressler et al., 1987; Djorgovski & Davis, 1987), wherein the stellar velocity dispersion is correlated with the luminosity and effective radius of an elliptical, further constrained the mechanisms responsible for galaxy formation. The fundamental plane can be reproduced in simulations of major mergers (Bekki, 1998; Nipoti et al., 2003; Boylan-Kolchin et al., 2005; Robertson et al., 2006; Hilz et al., 2012; Taranu et al., 2015), lending support to the theory of hierarchical structure formation through mergers of dark matter halos.

Similarly, galaxies are often found huddled together in groups (Zwicky, 1938, 1952; Abell, 1958), all sharing one large dark matter halo (groups with 100 or more galaxies are referred to as clusters Bower & Balogh 2004). Conversely some galaxies are found isolated from others in less dense environments (often referred to as the field), either because they are fossil groups (where all members have eventually merged Ponman et al., 1994; Jones et al., 2000, 2003) or have truly been isolated for their entire lifetimes. This environmental density is found to be correlated not only with morphology (Dressler, 1980; Smail et al., 1997; Poggianti et al., 1999; Postman et al.,

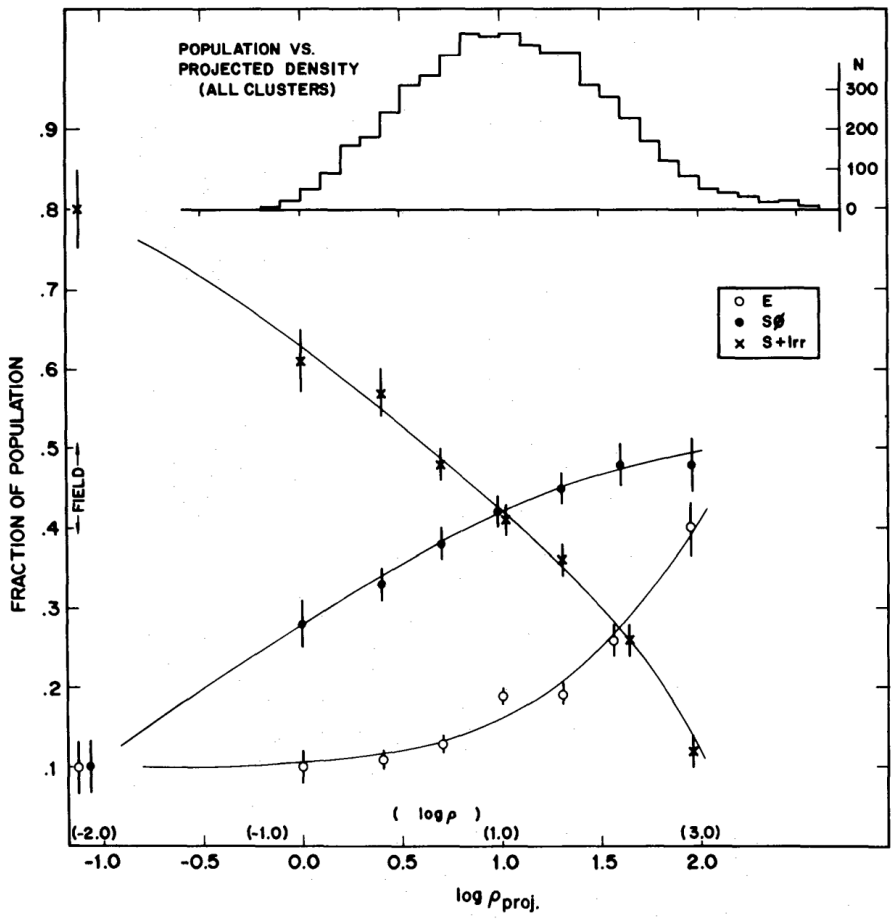

Figure 1.3: The morphology-density relation from Figure 4 of Dressler (1980) showing how the fraction of ellipticals (E) increases with increasing environmental density and the fraction of spirals (S + Irr) decreases.

2005; Bamford et al., 2009, and see Figure 1.3), but also colour (Butcher & Oemler, 1978; Pimbblet et al., 2002), quenched galaxy fraction (Kauffmann et al., 2003b; Baldry et al., 2006; Peng et al., 2012; Darvish et al., 2016) and SFR (Gómez et al., 2003) suggesting that the environment may drive this transition from blue cloud to red sequence due to the nature of hierarchical structure formation.

However, within this framework of hierarchical structure formation, the observed mass-metallicity relation (Tremonti et al., 2004) cannot be reproduced. This relationship describes how higher mass galaxies have higher metal contents. Simulations have shown that this phenomenon cannot be reproduced by the merging of galaxies alone, since mergers dilute the metallicity (Pipino & Matteucci, 2008; Rupke et al., 2010; Montuori et al., 2010; Torrey et al., 2012). This is also supported by observa-

tions showing that metallicities in galaxy pairs are suppressed by ~ 0.05 dex (Ellison et al., 2008; Michel-Dansac et al., 2008; Scudder et al., 2012). There must therefore be processes other than mergers occurring which are responsible for the colours, SFRs, masses, metallicities and morphologies of galaxies observed.

Further insight has also recently been revealed by the number of integral field unit (IFU) surveys which have come online in the past couple of years. These include the completed ATLAS^{3D} survey (Cappellari et al., 2011), which targeted a small sample of 260 early-type galaxies, and the larger, ongoing surveys of MaNGA (Bundy et al., 2015), SAMI (Croom et al., 2012) and CALIFA (Sánchez et al., 2012). Upon completion at the end of the decade, these surveys are expected to revolutionise the field of galaxy evolution, providing spatially resolved maps of the SFR in over $10,000$ galaxies.

Until that time, by studying galaxies which have just left the SFS sequence, the mechanisms governing galaxy evolution, including both the suppression of SF and the possible transformation of galaxy structure, can be revealed. Green valley galaxies have long been thought of as the 'crossroads' of galaxy evolution, a transition population between the two main galactic stages of the star forming blue cloud and the 'dead' red sequence. Bell et al. (2004) were the first to recognise that green valley galaxies may be a transitional population between the blue cloud and red sequence. Wyder et al. (2007) confirmed that galaxy bimodality also appears in NUV-optical colour space, with Schiminovich et al. (2007) investigating the morphological dependence in this parameter space and Martin et al. (2007) using it to constrain the flux of galaxies transitioning through the green valley. Faber et al. (2007) suggested that the build up of the red sequence has to occur via a mixture of suppression of star formation of galaxies in the blue cloud and mergers on the red sequence, which was confirmed by Mendez et al. (2011) who showed that mergers alone are not responsible for the transition from the blue cloud. This transition was theorised to occur on rapid timescales, otherwise there would be an accumulation of galaxies residing in the green valley (Gonçalves et al., 2012); however Schawinski et al. (2014) concluded that this was only true for elliptical galaxies, with disc galaxies transitioning much more slowly. The morphological dependence and causes of this transition are therefore still the cause of much debate.

I will refer to the suppression of a galaxy's SFR as *quenching* and processes which can cause this suppression as *quenching mechanisms*.

1.1 Possible quenching mechanisms

There are many theorised mechanisms which can cause quenching. They are often referred to as either *internal* mechanisms (caused by the galaxy's *nature*) or *external* mechanisms (caused by the way the galaxy is *nurtured*). The properties of a galaxy and its environment are often thought to control which mechanisms will affect a galaxy throughout its lifetime and subsequently affect the morphology.

1.1.1 Internal Quenching Mechanisms

1.1.1.1 AGN feedback as a quenching mechanism

An active galactic nucleus (AGN) is an actively growing supermassive black hole in the centre of a galaxy. There are many observed spectral classes of AGN which are explained by the viewing angle in the theory of unification (see review by Netzer, 2015). The basic structure of an AGN is an accretion disc of cold material which is formed around the black hole. The friction built up by the rotating gas causes the accretion disc to heat up and emit huge amounts of energy. The accretion disc is also surrounded by clouds of gas and an absorption region (often referred to as the torus) which can both re-emit and absorb the emitted light from the accretion disc (for a diagram depicting AGN structure see Beckmann & Shrader 2012). Type 2 Seyfert AGN are those which are viewed approximately edge on to their accretion disc and so have the majority of their emitted light absorbed by the torus. Some light is scattered off the surrounding gas clouds, resulting in the detection of broadened spectral emission lines. Type 1 Seyfert AGN however are those which are viewed perpendicular to their accretion disk and so are unobscured by the torus; light from both the accretion disc and/or emitted radiation jets can be observed.

There are tight correlations between properties of galaxies, such as the bulge mass, total stellar mass & stellar velocity dispersion, and the black hole mass (Magorrian et al., 1998; Marconi & Hunt, 2003; Häring & Rix, 2004). This implies a co-evolution between the black hole and its host galaxy therefore suggesting that changes in the SFR and structure of a galaxy could also be tied to black hole activity.

If we consider a 'back of the envelope' calculation of the ratio between the total

energy of the black hole and the binding energy of the galaxy, we can determine if output from the black hole will be able to have a significant effect on its host galaxy (see p.649 of Mo et al., 2010). The total energy output by a black hole in its lifetime can be expressed as $E_{BH} = \bar{\epsilon} M_{BH} c^2$, where $\bar{\epsilon}$ is the mean efficiency of the black hole of mass M_{BH}. The galaxy binding energy can be approximated as $E_{gal} \approx M_* \sigma^2$, where M_* is the stellar mass of the galaxy with stellar velocity dispersion σ. Taking the average values of $M_{BH} \sim 10^{8.0}$ $M_\odot$, $M_* \sim 10^{10.8}$ $M_\odot$ and $\sigma \sim 200$ km s^{-1} of the 30 galaxies observed by Häring & Rix (2004), we can estimate the ratio $E_{BH}/E_{gal} \sim \bar{\epsilon} 10^3$. The energy of the black hole can therefore easily surpass the binding energy of its galaxy, suggesting that a black hole can indeed impact its host. This is thought to occur via AGN feedback where the output of energetic material and radiation from the black hole is theorised to either heat or expel gas needed for SF in a galaxy, causing a quench. Energy from a black hole is observed to be ejected in narrow, collimated jets of material out of the plane of a galaxy (see review by Homan, 2012), but for AGN feedback to be effective these jets would somehow need to impact the gas in the entire galaxy.

AGN feedback was first suggested as a mechanism for regulating star formation due to the results of simulations wherein galaxies could grow to unrealistic stellar masses (Silk & Rees, 1998; Bower et al., 2006; Croton et al., 2006; Somerville et al., 2008). Without a prescription for the effects of AGN feedback, the shape of the galaxy luminosity function could therefore not be matched at the high luminosity end (Baugh et al., 1998, 2005; Kauffmann et al., 1999a,b; Somerville et al., 2001; Kitzbichler & White, 2006). A similar problem was also encountered at the low end of the luminosity function, which was rectified by the inclusion of the effects of supernova wind feedback (Dekel & Silk, 1986; Powell et al., 2011). This is illustrated in Figure 1.4 taken from Silk & Mamon (2012).

Indirect observational evidence has now been found for both positive and negative feedback in various systems (see the comprehensive review from Fabian 2012). The strongest being the indirect evidence that the largest AGN fraction is found in the green valley (Cowie & Barger, 2008; Hickox et al., 2009; Schawinski et al., 2010), suggesting a link between AGN activity and the process which moves a galaxy from the blue cloud to the red sequence. However, concrete statistical evidence for the effect of AGN feedback on the host galaxy population has so far been elusive.

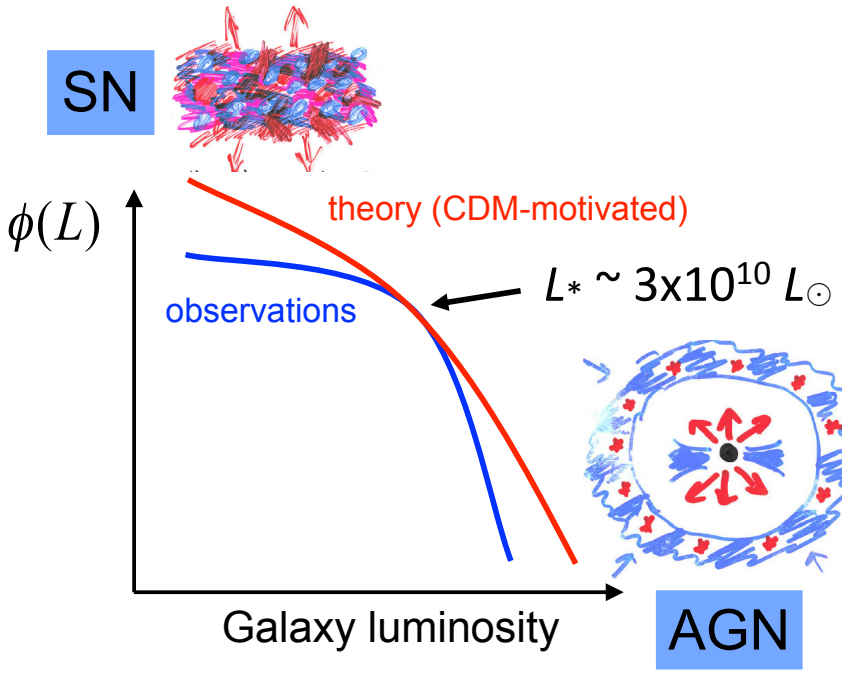

Figure 1.4: Cartoon of the role of feedback in modifying the observed luminosity function of galaxies with respect to theoretical predictions. Supernova winds are thought to be responsible at the low mass end, with AGN feedback responsible at the high mass end. Figure 1 in Silk & Mamon (2012).

1.1.1.2 Mass quenching

Mass quenching is defined by Peng et al. (2010, 2012) as any quenching mechanism which is independent of a galaxy's environment, but not of its mass. However, there is still much debate over the exact mechanism which is the cause of such a quench. Darvish et al. (2016) suggest that non-AGN driven feedbacks (for example supernova feedback) are responsible for the correlation observed between the mass quenching efficiency and SFR in Peng et al. (2010). However, Gabor & Davé (2015) suggest that this is driven by "halo quenching processes" whereby the inflow of cool gas from the galaxy halo is either cut off or hindered from cooling at $M_{halo} > 10^{12}$ $M_\odot$ (Birnboim & Dekel, 2003; Dekel & Birnboim, 2006). If this happens, a galaxy uses up the rest of its available gas for star formation via the Kennicutt-Schmidt law (Schmidt, 1959; Kennicutt, 1998) and consequently grows in mass.

In the rest of this thesis, I refer to mass quenching as a cut off of gas inflow,

resulting in a gradual consumption of gas in star formation. This definition of mass quenching is thought to be a dominant mechanism for isolated galaxies in the field (Kormendy & Kennicutt, 2004). However, it is also thought that as a galaxy infalls in to a group or cluster over long timescales, gas reservoirs can also be depleted via a mass quenching process (Peng et al., 2012).

1.1.1.3 Morphological quenching

Morphological quenching (or 'secular' quenching, referring to slow, non-violent processes) is the process by which the internal structure of a galaxy can have a negative impact on its own SFR[1]. This is theorised to occur in galaxies hosting bars; the bar funnels gas to the centre of the galaxy (Athanassoula, 1992a) where gas is exhausted by star formation effectively quenching the galaxy (Zurita et al., 2004; Sheth et al., 2005). This process is thought to be responsible for large numbers of red spirals and supported by observations of increasing bar fraction with red colours (Masters et al., 2011).

This process is also theorised to be caused by bulges (Bluck et al., 2014) whereby the large gravitational potential of the bulge prevents the disc from collapsing and forming stars (Fang et al., 2013). Recent observational evidence from Hart et al. (2016) also suggests that spiral structure can also cause morphological quenching. Hart et al. propose that many armed spiral structures can trigger galaxy wide starbursts thereby rapidly using up gas for future star formation; similarly two armed spirals are observed with redder colours, suggesting that this spiral phase is much longer lived and may funnel gas into the centre of the galaxy to be exhausted in star formation over longer timescales.

1.1.2 External Quenching Mechanisms

1.1.2.1 Mergers as a quenching mechanism

Major mergers have been intrinsically linked to the formation of elliptical galaxies since Toomre & Toomre (1972) showed this was possible with a simulation of the merger of two equal mass disc galaxies. Since Λ-CDM relies on the idea of hierarchical

[1]Essentially shooting itself in the foot.

structure formation through the merger of dark matter halos for its description of galaxy formation, it also follows that galaxy evolution should be further influenced by mergers.

The hypothesis is as follows. When two galaxies merge, the influx of cold gas funnelled by the forces in the interaction often results in energetic starbursts (Mihos & Hernquist, 1994, 1996; Hopkins et al., 2006a, 2008b,a; Snyder et al., 2011; Hayward et al., 2014; Sparre & Springel, 2016), which can exhaust the gas required for star formation, effectively quenching the post-merger remnant. This remnant galaxy will also have formed a dynamically hot bulge through the dissipation of angular momentum in the merger (Toomre, 1977; Walker et al., 1996; Kormendy & Kennicutt, 2004; Hopkins et al., 2012; Martig et al., 2012). The mass ratio of the two galaxies merging is thought to affect the size of the bulge that is formed in the remnant (Cox et al., 2008; Hopkins et al., 2009; Tonini et al., 2016), with the most massive major mergers with a 1:1 mass ratio producing fully elliptical galaxies (Toomre & Toomre, 1972; Barnes & Hernquist, 1996; Mihos & Hernquist, 1996; Kauffmann, 1996; Pontzen et al., 2016).

Such a scenario is also intrinsically linked to the triggering of an AGN due to the influx of gas in the merger which can fuel the black hole accretion (Sanders et al., 1988; Di Matteo et al., 2005; Hopkins & Hernquist, 2009; Treister et al., 2012). Many studies have therefore focussed on investigating the growth of black holes due to mergers (e.g. Veilleux et al., 2002; Bellovary et al., 2013; Ellison et al., 2013; Medling et al., 2015; Gabor et al., 2016). Simulations of mergers with AGN have lead many to believe that a merger which triggered both a starburst and an AGN can quench a galaxy in extremely rapid timescales (Springel et al., 2005; Bell et al., 2006). Recent simulations have also suggested that feedback from the triggered AGN (see Section 1.1.1.1) is necessary to fully remove (or heat) all the available gas, otherwise the SFR will recover back to the SFS post-merger (Pontzen et al., 2016; Sparre & Springel, 2016).

1.1.2.2 Environment driven quenching

The environment of a galaxy has long been considered a key *nurturing* aspect of galaxy evolution. Correlations of galaxy morphology (Dressler, 1980; Smail et al., 1997; Poggianti et al., 1999; Postman et al., 2005; Bamford et al., 2009), colour (Butcher &

Oemler, 1978; Pimbblet et al., 2002) and the quenched galaxy fraction (Kauffmann et al., 2003b; Baldry et al., 2006; Peng et al., 2012; Darvish et al., 2016) with the environmental density all suggest that the environment is in some way responsible for the build up of the red sequence through quenching.

The proposed quenching mechanisms under the umbrella of environmental quenching are numerous and varied. Together with the typical gravitational galaxy-galaxy interactions (Moore et al., 1996), including galaxy mergers which are expected to be more frequent in a dense environment, environmental quenching also includes hydrodynamic interactions occurring between the cold inter stellar medium (ISM) of the in-falling galaxy and the hot intergalactic medium (IGM) of the group or cluster. Such hydrodynamic interactions include ram pressure stripping (Gunn & Gott, 1972), viscous stripping (Nulsen, 1982), and thermal evaporation (a rapid rise in temperature of the ISM due to contact with the IGM; Cowie & Songaila, 1977). Another such process is starvation (Larson et al., 1980) which can remove the outer galaxy halo cutting off the star formation gas supply to a galaxy. Preprocessing occurs when all of the above mechanisms take place in a group of galaxies which then merges with a larger group or cluster (Dressler, 2004).

The most likely candidate (and therefore the most studied) mechanism for the cause of the environmental density-morphology and SFR relations is ram pressure stripping (RPS; Abadi et al., 1999; Poggianti et al., 1999). However, there has been mounting evidence that RPS can only strip a galaxy of $40 - 60\%$ of its gas supply (Fillingham et al., 2016) and so may not be as effective of a quenching mechanism as first thought (Emerick et al., 2016). Therefore investigations of other environmentally driven quenching mechanisms, such as strangulation (Peng et al., 2015; Hahn et al., 2016; Maier et al., 2016; Paccagnella et al., 2016; Roberts et al., 2016; van de Voort et al., 2016) and harassment (Bialas et al., 2015; Smith et al., 2015a) are having a recent resurgence.

1.2 Using star formation histories to investigate quenching

In order to understand how a galaxy is quenched, the star formation history (SFH) is often modelled. This approach requires the inference of the global SFH of a galaxy

from a its current stellar population. While in nearby galaxies it is possible to observe resolved stellar populations with the Hubble Space Telescope (HST) to pinpoint the main sequence turn off (an indicator of the age of a stellar population) on the Hertzsprung Russel diagram, this is not possible in more distant galaxies. Instead, reliance is placed upon the correlation between the integrated total light of a galaxy and its SFH (Searle et al., 1973). Adopting a global SFH for a galaxy is a big assumption, especially since recent IFU studies have shown that bulges and discs have vastly different SFHs (see for example Johnston et al., 2016). However, these differences will smear out across the integrated light of a galaxy and so inferring the SFH in this way will give an estimate of the average global SFH of the galaxy.

Many studies have employed this technique using either photometric broadband colours or spectral data as indicators of the integrated SFH (for example de Jong, 1996; Madau et al., 1998; Kauffmann et al., 2003b; Dressler, 2004; MacArthur et al., 2004; Martin et al., 2007; Pérez & Sánchez-Blázquez, 2011; Sánchez-Blázquez et al., 2011; McDermid et al., 2015). However, this technique is sensitive to the degeneracies between age and metallicity (Worthey, 1994) and the effects of dust (Ganda et al., 2009; Pastrav et al., 2013) on the integrated light.

The turn of the millennium therefore saw the development of full spectral energy density (SED) fitting codes to infer the SFH (without having to make any prior assumptions on its form) such as MOPED (Heavens et al., 2000), STARLIGHT (Cid Fernandes et al., 2005), VESPA (Tojeiro et al., 2007), and more recently FIREFLY (Wilkinson, 2015). In the absence of spectral data however, broadband colours are still effective at inferring the global SFHs of galaxies, especially when wavebands across the spectrum, such as ultra-violet, optical and infrared colours, are used simultaneously (Madau et al., 1998).

This method is achieved by modelling the observed SED of a galaxy using a combination of SEDs of simple stellar populations (SSP) at various ages. SSPs assume stars are coeval and form with the same metallicity and comprehensive knowledge of stellar evolutionary tracks and initial mass functions (IMF; Salpeter, 1955; Chabrier, 2003) are therefore needed to calculate the spectrum of a SSP at a given age (Chen et al., 2010; Kriek et al., 2010). Luckily, some astronomers have made the study of these SSPs their life's work (Bruzual & Charlot, 2003; Maraston, 2005; Vázquez & Leitherer, 2005; Conroy et al., 2009, for example), therefore once an IMF and a SFH function have been assumed, the SED of a model galaxy can be predicted at any

point in its history (Chen et al., 2010). This technique also assumes a universal IMF, which recent studies have shown may not be appropriate (van Dokkum, 2008; Conroy & van Dokkum, 2012; Cappellari et al., 2012; Smith et al., 2015b). Whilst the choice of an IMF and metallicity of a SSP will affect the output SED (Conroy et al., 2009; Kriek et al., 2010), the choice of the functional form of the SFH will have the greatest impact.

Many possible forms for global galaxy SFHs have been assumed in previous studies, including an exponential decline (Tinsley, 1972; Gavazzi et al., 2002; Weiner et al., 2006; Martin et al., 2007; Noeske et al., 2007; Kriek et al., 2010; Schawinski et al., 2014; Hart et al., 2016), the extended (or delayed) exponential model (Gavazzi et al., 2002; Oemler et al., 2013; Simha et al., 2014), a Gaussian distribution (Feuillet et al., 2016) or a log normal distribution (Gladders et al., 2013; Abramson et al., 2016). These models are by no means a perfect description of a galaxy's SFH (Lee et al., 2010; Boquien et al., 2014; Smith & Hayward, 2015), as they generalise the localised bursts of SF across a galaxy's lifetime into a global SFH, but they still allow some insight to be gained on the complex processes responsible for the SFHs seen across the galaxy population.

In this thesis I will assume an exponentially declining SFH for galaxies with morphological classifications from Galaxy Zoo. Using Bayesian methods, I will use optical and NUV photometry to infer the dependence of quenching histories on the morphology across the colour magnitude diagram. I will also investigate the quenching histories of galaxies hosting AGN and those in dense environments to help constrain the quenching mechanisms responsible for galaxy evolution.

1.3 Data

In the following section I describe the data sources for the optical & NUV colours and morphologies used throughout this study.

1.3.1 Sloan Digital Sky Survey

The Sloan Digital Sky Survey (SDSS; York et al. 2000) is an optical imaging and spectroscopic survey of $8,000$ square degrees of sky, which was completed using a 2.5m telescope at Apache Point Observatory in New Mexico, USA. SDSS Data Release 8 (Aihara et al., 2011) provided publicly available optical magnitudes across 5 broadband filters, *ugriz* for over 1 million galaxies in the 'main galaxy' sample. Here I utilise the Petrosian magnitudes, `petroMag`, values for the u ($3,543$Å) and r ($6,231$Å) wavebands provided by the SDSS pipeline. Spectral data is available for a significant proportion of the SDSS main galaxy sample but the spectral fibre is a set size. Therefore across a population of galaxies the fibre will cover varying radii at different distances and of different sizes. Therefore the usual spectral star formation indicators cannot be utilised in this study as they will over- or under-estimate the global average SFR of a galaxy.

Magnitudes are corrected for galactic extinction (Oh et al., 2011) by applying the Cardelli et al. (1989) law, giving a typical correction of $u - r \sim 0.05$. K-corrections are also adopted to $z = 0.0$ and absolute magnitudes obtained from the NYU-VAGC (Blanton et al., 2005; Padmanabhan et al., 2008; Blanton & Roweis, 2007), giving a typical $u - r$ correction of ~ 0.15 mag. The change in the $u - r$ colour due to both corrections therefore ranges from $\Delta(u - r) \sim 0.2$ at low redshift, increasing up to $\Delta(u - r) \sim 1.0$ at $z \sim 0.25$, which is consistent with the expected k-corrections shown in Figure 15 of Blanton & Roweis (2007). These corrections were calculated by Bamford et al. (2009) for a subset of galaxies in the SDSS survey. These corrections are a crucial aspect of this work since a $\Delta(u - r) \sim 1.0$ can cause a galaxy to change whether it is class as blue cloud, green valley or red sequence.

Star formation rates and stellar masses, where available, were obtained from the MPA-JHU catalog (Kauffmann et al., 2003b; Brinchmann et al., 2004). These SFRs are derived from emission lines using the method of Charlot & Longhetti (2001). All SFRs are corrected for aperture size by fitting to the photometry outside the fibre with stochastic models as in Salim et al. (2007). SFRs for non star forming galaxies and AGN were derived indirectly using the $4,000$Å break. Those galaxies with emission lines with low signal-to-noise ratio, the SFR was estimated indirectly using a conversion factor likelihood distribution between the luminosity of the Hα Balmer emission line and the SFR. Masses are obtained from fits to the photometry with a large grid of SFHs produced using the Bruzual & Charlot (2003) models. In

this thesis these values are obtained for interest to compare samples; they are never used to infer the SFHs of galaxies due to the circular nature of the modelling used to derive the values. I use the average values of AVG SFR and AVG MASS from the inferred likelihood distributions for each galaxy.

1.3.2 Galaxy Evolution Explorer

The Galaxy Evolution Explorer (GALEX; Martin et al. 2005) is an ultra-violet space based telescope which imaged galaxies simultaneously in two broadband filters: both the far ultra-violet (FUV) with an effective wavelength of $1,516$Å and in the NUV with an effective wavelength of $2,267$Å. Sources detected with GALEX were matched with a search radius of $1''$ to the SDSS data in right ascension and declination. The `auto` magnitudes provided by the GALEX pipeline are used in this study (for a discussion of aperture bias between different surveys see Hill et al. 2011). All magnitudes are k-corrected and extinction corrected as described in Section 1.3.1.

1.3.3 Galaxy Zoo

Galaxy Zoo (GZ) is a citizen science project enlisting the help of thousands of members of the public to voluntarily classify galaxy images online[2]. The first version of GZ classified just under 1 million SDSS galaxy images as either ellipticals, spirals or mergers within approximately 6 months of launch (Lintott et al., 2008, 2011). In the second version, GZ2 (Willett et al., 2013), volunteers were asked to make more detailed morphological classifications of $304,022$ images from the SDSS DR8 (a subset of those classified in the first Galaxy Zoo; GZ1). These images were all classified by *at least* 17 independent volunteers, with the mean number of classifications standing at ~ 42. GZ is now in its tenth year of classifying and its fifth incarnation, after classifying images from Hubble Space Telescope Legacy surveys in GZ:Hubble (Willett et al., 2016) and the CANDELS survey galaxies in GZ:CANDELS (Simmons et al., 2016). At the time of writing, images from the DeCALS[3] survey and Illustrius simulation (Vogelsberger et al., 2014; Genel et al., 2014) are being classified by volunteers.

[2] `http://galaxyzoo.org`
[3] `http://legacysurvey.org/`

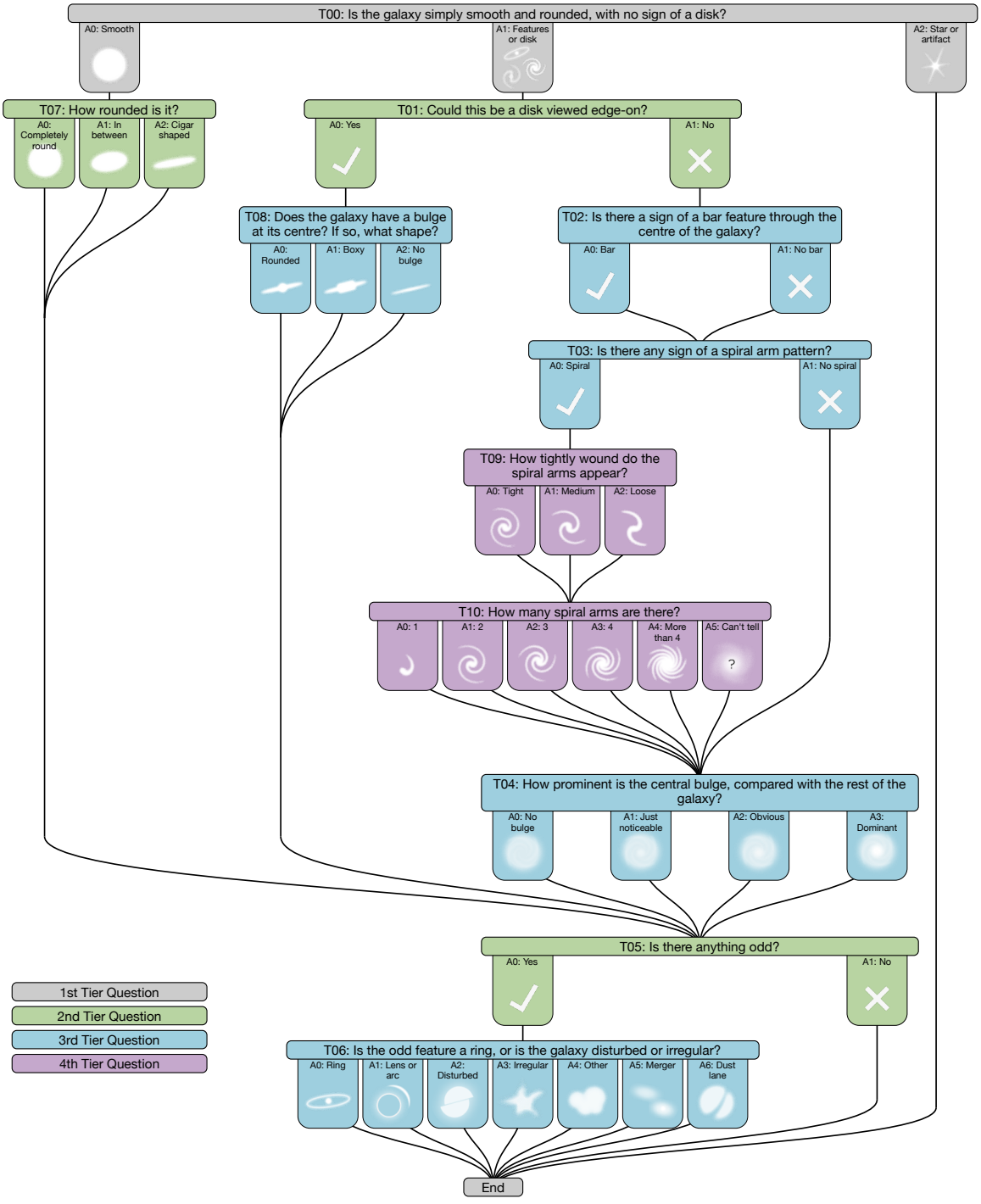

Figure 1.5: Flowchart of the classification tree for GZ2, beginning at the top with Task 0. Tasks are colour-coded by their relative depths in the decision tree with tasks in green, blue and purple respectively one, two or three steps below branching points in the decision tree.

From GZ2 onwards, all projects have collected classification data via a multi-step decision tree, shown in Figure 1.5. Each individual step in a tree is a *task*, which consists of a *question* with a finite number of possible *answers*. The selection of an answer is called the volunteer's *vote*. The first task of GZ2 asks volunteers to choose whether a galaxy is mostly smooth, is featured and/or has a disc or is a star/artefact. Every volunteer who classifies a galaxy image will complete this task, therefore the most statistically robust classifications are available at this level.

The classifications from volunteers produces a vote fraction for each galaxy; for example if 80 of 100 people thought a galaxy was featured and/or had a disc, whereas 20 out of 100 people thought the same galaxy was mostly smooth (i.e. elliptical), that galaxy would have raw vote fractions $p_s = 0.8$ and $p_d = 0.2$. In this example this galaxy would be included in the *'clean'* disc sample ($p_d \geq 0.8$) according to Willett et al. (2013) and would be considered a late-type galaxy. Similar vote fractions can be produced at each stage in the tree, such as $\{p_{\rm bar}, p_{\rm no\ bar}\}$, $\{p_{\rm spiral}, p_{\rm no\ spiral}\}$ and $\{p_{\rm odd}, p_{\rm not\ odd}\}$. Selecting a sample of galaxies with a specific feature using these vote fractions becomes a trade off between purity and completeness. Since not every volunteer will submit a response to a 2nd, 3rd or 4th tier question (see Figure 1.5), the number of classifiers recording a response must be considered, in order to reduce noise in cases where only a small number of people answered that task.

For example imagine that a galaxy is classified by 40 people, 38 of whom say that the galaxy is mostly smooth in answer to the first question. However, 2 people decide that the galaxy is featured and/or has a disc, both of whom subsequently respond to Task 2 to say that there is a sign of a bar in the same galaxy. This would give a $p_{\rm bar} = 1$, despite the fact that the $p_s = 0.95$. This is an unlikely situation, but highlights the need for not only consideration of the number of respondents for a task but also the vote fractions of previous tasks when using a threshold to identify a subset of features. Appropriate values for these thresholds given the number of respondents are shown in Table 1.1 (reproduced from Table 3 in Willett et al. 2013) and are adopted where relevant throughout this study.

All previous Galaxy Zoo projects have also incorporated extensive analysis of volunteer classifications to measure classification accuracy and bias. A weighting is computed for each volunteer based on their classification history and the redshit of each galaxy considered in order to produce debiased vote fractions for each galaxy (for

Task	Previous task	Vote fraction $N_{task} \geq 10$	Vote fraction $N_{task} \geq 20$
00	–	–	–
01	00	0.227	0.430
02	00,01	0.519	0.715
03	00,01	0.519	0.715
04	00,01	0.519	0.715
05	–	–	–
06	05	0.263	0.469
07	00	0.223	0.420
08	00,01	0.326	0.602
09	00,01,03	0.402	0.619
10	00,01,03	0.402	0.619

Table 1.1: Thresholds for determining well-sampled galaxies in GZ2. Thresholds depend on the number of respondents for a task, including the thresholds that should be applied to previous task(s) for both 10 and 20 respondents. As an example, to select galaxies that may or may not contain bars, cuts for $p_{\text{features/disc}} > 0.430$, $p_{\text{not edgeon}} > 0.715$, and $N_{\text{not edgeon}} \geq 20$ should be applied. No thresholds are given for Tasks 01 and 06, since these are answered for every classification in GZ2. The task numbers are those defined in Figure 1.5.

a detailed description of redshift debiasing and consistency-based volunteer weightings, see either Section 3 of Lintott et al. 2009 or Section 3 of Willett et al. 2013). This produces highly accurate and robust detailed morphological classifications and is a significant statistical improvement over efforts completed using only a small number of expert classifiers (Schawinski et al., 2007b; Nair & Abraham, 2010a; Ann et al., 2015). These classifications can now be used as machine learning training sets (Dieleman et al., 2015) to improve future automated classifications of galaxies.

The debiased GZ2 p_d and p_s vote fractions encompass the continuous spectrum of morphological features (as shown in Figure 1.6), rather than a simple binary classification separating elliptical and disc galaxies (see Section 6.1). These classifications allow each galaxy to be considered as a probabilistic object with both bulge and disc components. I utilise the debiased GZ2 vote fractions in this study to facilitate future work studying more detailed galaxy structures.

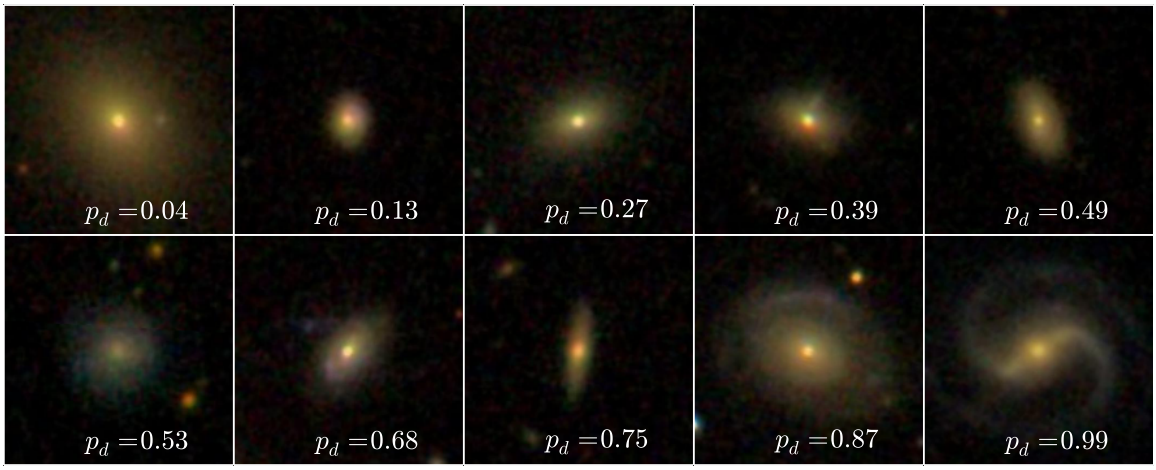

Figure 1.6: Randomly selected SDSS *gri* composite images showing the continuous probabilistic nature of the Galaxy Zoo sample from a redshift range $0.070 < z < 0.075$. The debiased disc vote fraction for each galaxy is shown. The scale for each image is 0.099 arcsec/pixel.

1.3.4 Defining the GZ2-GALEX main galaxy sample

I require a sample of galaxies with optical and NUV photometry from SDSS and GALEX respectively, along with morphologies from GZ2 in order to study the morphological dependence of galaxy quenching histories. The GZ2 sample consists of $304,022$ SDSS galaxies which were selected to include the brightest ($m_r < 17$), largest (radius containing 90% of the Petrosian flux, $r_{90} > 3''$) and nearest ($0.005 < z < 0.25$) galaxies in order to achieve robust detailed morphological classifications. I first removed those objects considered to be stars or artefacts in Task 0 or merging pairs in Task 6 (using the thresholds defined in Table 1.1) from this GZ2 sample. Further to this, I required NUV photometry from the GALEX survey, within which $\sim 42\%$ of the GZ2 sample galaxies were observed, giving a total sample size of $126,316$ galaxies. This will be referred to as the GZ2-GALEX sample.

The completeness of the GZ2-GALEX sample is shown in Figure 1.7 with the u-band absolute magnitude against redshift, compared with the SDSS data set. Despite the GZ2 selection for the brightest and largest galaxies and the cross match to GALEX (which has a higher magnitude limit than SDSS) typical Milky Way L_* galaxies with $M_u \sim -20.5$ are still included in the GZ2 subsample out to the highest redshift of $z \sim 0.25$; however dwarf and lower mass galaxies are only detected at the lowest redshifts. The redshift is taken into account during the SFH modelling (see Section 2.1).

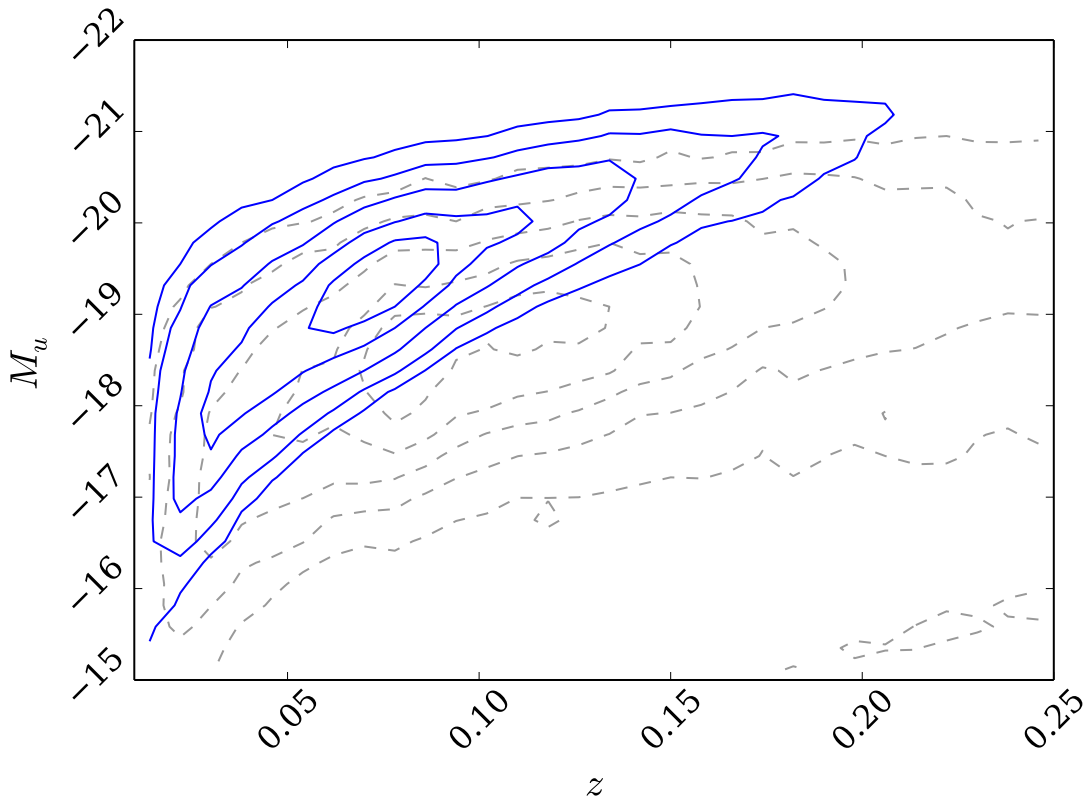

Figure 1.7: Absolute u-band magnitude against redshift for the whole of SDSS (grey dashed lines) in comparison to the GZ2 subsample (blue solid lines). Typical Milky Way L_* galaxies with $M_u \sim -20.5$ are still included in the GZ2 subsample out to the highest redshift.

Galaxy colours were not corrected for intrinsic dust attenuation. This is of particular consequence for disc galaxies, where attenuation increases with increasing inclination. Buat et al. (2005) found the median value of the attenuation in the GALEX NUV passband to be ~ 1 mag. Similarly Masters et al. (2010b) found a total extinction from face-on to edge-on spirals of 0.7 and 0.5 mag for the SDSS u and r passbands and show spirals with $\log(a/b) > 0.7$ have signs of significant dust attenuation. For the GZ2-GALEX sample I find $\sim 29\%$ of discs (with $p_d > 0.5$) have $\log(a/b) > 0.7$, therefore we must be aware of possible biases in the results due to dust.

I shall use the GZ2-GALEX sample to probe how different quenching mechanisms cause galaxies of different morphologies and environments to transition from the SFS to quiescence.

1.4 Thesis Summary

This thesis proceeds as follows. In Chapter 2 I describe the SFH model used to characterise the colours of quenching galaxies, along with the statistical methods used to determine the distribution of quenching histories in a population of galaxies. In Chapter 3 I apply this method across the red sequence, green valley and blue cloud and investigate the morphological dependence of quenching histories in these populations. Chapter 4 is split into two parts. In Section 4.1 I investigate the effect of AGN feedback on the quenching histories of a population of AGN host galaxies. In Section 4.2 I investigate the proposed slow co-evolution of galaxies with their central black holes, by measuring the black hole masses of a sample of bulgeless galaxies, which have assumed merger free histories. In Chapter 5 I return to investigating the quenching histories of galaxies, this time focussing on the effect of the group environment on satellite galaxies in comparison to centrals and those in the field. In Chapter 6 I discuss how the implications of my results in the context of galaxy evolution and propose ideas for future work.

Where necessary I adopt the Planck 2015 cosmological results (Planck Collaboration, 2016) with $(\Omega_m, \Omega_\lambda, h) = (0.309 \pm 0.006, 0.691 \pm 0.006, 0.677 \pm 0.005)$.